

# A Fission Yeast Gene for Mitochondrial Sulfide Oxidation\*

(Received for publication, December 2, 1998, and in revised form, February 24, 1999)

Jennifer G. Vande Weghe<sup>†§¶</sup> and David W. Ow<sup>‡¶</sup>

From the <sup>‡</sup>Plant Gene Expression Center, U. S. Department of Agriculture-Agricultural Research Service, Albany, California 94710 and the <sup>§</sup>Department of Plant and Microbial Biology, University of California, Berkeley, California 94720

**A cadmium-hypersensitive mutant of the fission yeast *Schizosaccharomyces pombe* was found to accumulate abnormally high levels of sulfide. The gene required for normal regulation of sulfide levels, *hmt2*<sup>+</sup>, was cloned by complementation of the cadmium-hypersensitive phenotype of the mutant. Cell fractionation and immunocytochemistry indicated that HMT2 protein is localized to mitochondria. Sequence analysis revealed homology between HMT2 and sulfide dehydrogenases from photosynthetic bacteria. HMT2 protein, produced in and purified from *Escherichia coli*, was soluble, bound FAD, and catalyzed the reduction of quinone (coenzyme Q<sub>2</sub>) by sulfide. HMT2 activity was also detected in isolated fission yeast mitochondria. We propose that HMT2 functions as a sulfide:quinone oxidoreductase. Homologous enzymes may be widespread in higher organisms, as sulfide-oxidizing activities have been described previously in animal mitochondria, and genes of unknown function, but with similarity to *hmt2*<sup>+</sup>, are present in the genomes of flies, worms, rats, mice, and humans.**

The oxidation of sulfide can provide energy for chemolithotrophic or photosynthetic growth of bacteria. This capacity allows some bacteria to thrive in such unlikely environments as hot sulfur springs and deep-sea thermal vents. Sulfide-based anoxygenic photosynthesis appeared quite early in evolution. Today, it is widespread in the green and purple phototrophic bacteria and has been reported in cyanobacteria (1). Enzymes mediating sulfide oxidation have been described in the photosynthetic bacteria *Chlorobium limicola* (2, 3), *Oscillatoria limnetica* (4), *Rhodobacter capsulatus* (5), and *Chromatium vinosum* (6); the complete sequence of the latter two proteins has been described.

In recent years, it has become known that sulfide oxidation is not the province solely of bacteria. Some animals from sulfide-rich aquatic sediments, such as the gutless clam (*Solemya reidi*) and the lugworm (*Arenicola marina*) are able to oxidize sulfide within their own tissues without the aid of bacterial symbionts (7–12). This capacity allows them to detoxify sulfide that enters their bodies from the surrounding environment

that would otherwise poison aerobic metabolism. The enzymes responsible for sulfide oxidation in these eukaryotes have not been isolated, and their nature and evolutionary origin remain unknown. In particular, it is not clear if sulfide oxidation in this exotic group of organisms bears any relationship with the better-understood pathways of bacteria.

The lower eukaryote *Schizosaccharomyces pombe* (fission yeast) has not been described to live in sulfide-rich habitats, although cells are exposed to sulfide generated internally during assimilation of inorganic sulfur. After reduction of sulfate to sulfite over several steps, the enzyme sulfite reductase catalyzes the reaction [H<sub>2</sub>SO<sub>3</sub> + 3 NADPH + 3H<sup>+</sup> → S<sup>2-</sup> + 3 NADP<sup>+</sup> + 3 H<sub>2</sub>O]. Much of this S<sup>2-</sup> is incorporated into cysteine, but the cell still accumulates measurable amounts of acid-labile S<sup>2-</sup> under normal laboratory conditions. S<sup>2-</sup> increases during exposure to heavy metals and is involved in resistance to cadmium and cisplatin (13).

In the course of studying the response of fission yeast to heavy metals, we uncovered a mutant with an unusual defect in sulfur metabolism. This led to the cloning and characterization of a new gene encoding a mitochondrial enzyme that can oxidize sulfide. The protein has sequence homology to sulfide-oxidizing enzymes of bacterial photosynthesis, suggesting a common evolutionary origin of sulfide metabolism between prokaryotes and eukaryotes. Interestingly, potential homologues of this enzyme appear in the genomes of nematodes, fruit flies, mice, rats, and humans. This raises the possibility that sulfide oxidation is more widespread among organisms, and might occur in a wider diversity of habitats, than has previously been imagined.

## EXPERIMENTAL PROCEDURES

**Genetic Materials**—*S. pombe* strains Sp223 (*h*<sup>-</sup>, *ade6.216*, *ura4.294*, *leu1.32*) and B1048 (*h*<sup>+</sup>, *ade7.50*, *ura4.294*) have been described (14). JS21 (*h*<sup>-</sup>, *ura4.294*, *leu1.32*) and JS23 (*h*<sup>+</sup>, *ura4.294*, *leu1.32*) were derived from the mating of Sp223 with B1048. A cadmium-hypersensitive mutant of JS21 was crossed to JS23 to yield JS563 (*h*<sup>+</sup>, *ura4.294*, *leu1.32*, *hmt2*<sup>-</sup>) and JV7 (*h*<sup>-</sup>, *ura4.294*, *leu1.32*, *hmt2*<sup>-</sup>). JV5 (*h*<sup>-</sup>, *ura4.294*, *leu1.32*, *hmt2::URA3*<sup>+</sup>) harbors a homologous insertion, whereas JV11 (*h*<sup>-</sup>, *ura4.294*, *leu1.32*, *URA3*<sup>+</sup>) harbors a random insertion of an *hmt2*<sup>-</sup> disruption construct bearing the *Saccharomyces cerevisiae* *URA3*<sup>+</sup> gene. DS31 (*h*<sup>+</sup>, *ura4.294*, *leu1.32*, *sir1::LEU2*) was generated by disruption of the sulfite reductase gene with a *S. cerevisiae* *LEU2*<sup>+</sup> fragment (D. Speiser, USDA-ARS, Albany, CA). JV3 (*ura4.294*, *leu1.32*, *sir1::LEU2*, *hmt2*<sup>-</sup>) was obtained from the mating of DS31 with JV7.

**Growth Conditions**—Cells were grown at 30 °C on complete medium YG (2% glucose, 0.5% yeast extract) or minimal medium SG (2% glucose, 0.67% yeast nitrogen base without amino acids; supplemented with 20 μg/ml uracil and/or 100 μg/ml leucine as needed). JS21 cells were mutagenized by a 45-min exposure to 175 μg/ml MNNG.<sup>1</sup> Media for comparison of growth on glucose or glycerol consisted of either 1% yeast extract, 2% glucose or 1% yeast extract, 4% glycerol, 0.1% glucose,

\* This work was supported by U. S. Department of Energy Grant EM96–55278 (to D. W. O.). The costs of publication of this article were defrayed in part by the payment of page charges. This article must therefore be hereby marked “advertisement” in accordance with 18 U.S.C. Section 1734 solely to indicate this fact.

The nucleotide sequence(s) reported in this paper has been submitted to the GenBank™/EMBL Data Bank with accession number(s) AF042283.

¶ Present address: MicroGenomics Inc., 11211 Sorrento Valley Rd., San Diego, CA 92121.

‡ To whom correspondence should be addressed: Plant Gene Expression Center, USDA-ARS, 800 Buchanan St., Albany, CA 94710. Tel.: 510-559-5909; Fax: 510-559-5678; Email: ow@pgec.ars.usda.gov.

<sup>1</sup> The abbreviations used are: MNNG, *N*-methyl-*N'*-nitro-*N*-nitrosoguanidine; DTNB, 5,5'-dithiobis(2-nitrobenzoic acid); CHAPS, 3-[(3-cholamidopropyl)dimethylammonio]-1-propanesulfonic acid; kb, kilobase(s); IPTG, isopropyl-1-thio-β-D-galactopyranoside.

respectively.

**Sulfide Analysis**— $S^{2-}$  was collected and assayed as described (14).  $S^{2-}$  content was first normalized to the dry weight of the cell culture and, to minimize day-to-day assay variability, was subsequently normalized to each day's value obtained from wild-type cells grown without cadmium (set to 1.0).

For  $^{35}S$ -labeling of sulfide *in vivo*, cells incubated for 20 min in 4 ml of low sulfur medium (MM medium (15) minus sodium sulfate) were spiked with 80  $\mu$ Ci  $Na_2^{35}SO_4$ . After 15 min, the cells were harvested, washed with phosphate-buffered saline, and resuspended in 200 ml of YG containing 200  $\mu$ M cadmium. Cells at various time points were collected and frozen in liquid nitrogen for high performance liquid chromatography analysis.

For analysis of  $S^{2-}$  turnover, labeled cell pellets were homogenized and centrifuged for 2 min at  $15,000 \times g$ , 4 °C. Proteins were precipitated with 5% 5-sulfosalicylic acid. After filtration of supernatants, samples were injected onto a Betasil Basic-18 high performance liquid chromatography column (Keystone Scientific) equilibrated in 5% acetonitrile, 95% 0.05% trifluoroacetic acid in water, and eluted by a linear gradient to 12.5% acetonitrile, 87.5% (0.05% trifluoroacetic acid in water) over 20 min, at a rate of 1 ml/min. 0.7 mg/ml DTNB in 0.3 M  $KPO_4$ , pH 7.8, 7.5 mM EDTA was mixed with post-column effluent at a rate of 0.1 ml/min, and absorption of the derivatized effluent was monitored at 405 nm. Effluent was then mixed with an equal amount of Ultima-Flo M scintillation mixture (Packard Instrument), and radioactive peaks were monitored by flow scintillation counting.  $Na_2S$  was used as a standard for peak identification and quantification.

**Molecular Cloning**—*S. pombe* genomic and cDNA libraries were described previously (16). Transformation of *S. pombe* was performed essentially as described (17). For gene disruption, the *EcoRV* to *SphI* fragment of pJV1, containing part of the *hmt2*<sup>+</sup> coding sequence, was replaced by the *S. cerevisiae* *URA3*<sup>+</sup> gene. A linear 4.1-kb *XbaI* fragment from this pJV17 plasmid was transformed into JS21, and colonies prototrophic for uracil were selected. For Northern analysis of *hmt2*<sup>+</sup> expression, RNA was prepared as described (16). Blots were hybridized to random primer-labeled *hmt2*<sup>+</sup> cDNA and, following stripping of the blot, were reprobated with an end-labeled oligonucleotide representing a short antisense sequence of the *S. pombe* 18 S rRNA. The mutant *hmt2*<sup>-</sup> allele was cloned into pART1 (18) to form pJV30. A 300-base pair *HindIII* to *ScaI* fragment containing the mutation was replaced with wild-type DNA to form pJV34.

pJV37 contains the *hmt2*<sup>+</sup> coding sequence in the pQE12 *Escherichia coli* expression vector (Qiagen). The *hmt2*<sup>+</sup> genomic clone was cleaved with *PacI*. Ends were made flush with T4 DNA polymerase and ligated to *BglII* linkers. The DNA was cleaved with *BglII*, followed by *HincII* that released a fragment containing all but the first two and the last codons of *hmt2*<sup>+</sup>. This fragment was ligated to pQE12 that had been cleaved with *BamHI*, made flush with the Klenow fragment of DNA polymerase I, and subsequently cleaved with *BglII*. The resulting construct encodes an *hmt2*<sup>+</sup> fusion protein having four new vector-derived N-terminal amino acids and nine new vector-derived C-terminal amino acids, the last 6 of which are histidines. The DNA encoding the entire fusion protein from pJV37 was cloned into pART1 under the control of the alcohol dehydrogenase promoter to form pJV40. This construct was transformed into JS563, and cadmium sensitivity was compared with JS563 and JS23 containing the empty vector pART1.

**Cell Fractionation**—Cells grown in SG were vortexed with glass beads in an equal volume of 10 mM Tris-Cl, pH 7, 0.15 M NaCl, 0.25 M sucrose, 1 mM each phenylmethylsulfonyl fluoride, EDTA, EGTA, dithiothreitol, and benzamidine HCl. Unbroken cells and debris were removed by centrifugation at  $1,000 \times g$  for 10 min. The total protein preparation was further fractionated by centrifugation at  $100,000 \times g$  for 1 h. Protein was quantified using an assay kit (Bio-Rad) in the presence of 0.05% CHAPS for membrane-containing samples.

Mitochondria were isolated using published procedures (19, 20). Marker enzymes corresponding to various cell compartments were assayed: cytochrome *c* oxidase (mitochondria), cytochrome *c* reductase (endoplasmic reticulum),  $\alpha$ -mannosidase (vacuole), glucose-6-phosphate dehydrogenase (cytoplasm), catalase (peroxisome), and guanosine diphosphatase (Golgi). The results indicated that mitochondria were ~6-fold enriched over their initial abundance in the cell homogenate, whereas the abundance of other organelles was decreased or relatively unchanged. Mitochondrial subfractionation was carried out with minor modifications from a published protocol (21). Activity of the soluble matrix enzyme fumarase (22) was used to monitor mitochondrial breakage. For investigation of the effects of pH on HMT2 solubility, mitochondria were suspended in ice-cold 0.6 M sucrose, 3 mM  $MgCl_2$ , 20 mM Tris-Cl, pH 7.4, or 0.6 M sucrose, 3 mM  $MgCl_2$ , 20 mM

$Na_2CO_3$ , pH 11. Mitochondria were sonicated for a total of 4 min, with rest periods on ice, then centrifuged for 1 h at  $100,000 \times g$ .

**Antibody Production and Immunodetection**—HMT2 protein was purified under denaturing conditions from XL1-Blue *E. coli* (Stratagene) carrying pJV37, according to the QIAexpress kit protocol (Qiagen). Purified protein was electroeluted from a preparative SDS-polyacrylamide electrophoresis gel, mixed with MPL+ TDM + CWS Emulsion (RIBI ImmunoChem Research), and used to immunize two rabbits. For Western blots, anti-HMT2 antisera were typically used at a dilution of 1/30,000. Chemiluminescent detection of Western blots has been described (23). The polyclonal antisera specifically recognize the recombinant protein in Western blots of extracts from *E. coli* expressing tagged HMT2, but not from *E. coli* bearing the empty expression vector.

**Nondenaturing Protein Purification**—*E. coli* XL1-Blue carrying pJV37 was grown to  $A_{600} = 0.6$  at 30 °C in 4 liters of LB, 1 M sorbitol, 2.5 mM betaine, 50  $\mu$ g/ml carbenicillin, and induced for 2.5 h with 1 mM IPTG. Cells were harvested by centrifugation and resuspended in 100 ml of 50 mM  $NaPO_4$ , pH 7.8, 50 mM NaCl, 10% glycerol, 0.1% Triton X-100. After incubation with 0.1 mg/ml lysozyme on ice for 15 min and three rapid freeze-thaw cycles, extracts were sonicated briefly and centrifuged at  $10,000 \times g$  for 20 min. The supernatant was applied to a DEAE-Sephadex column (Amersham Pharmacia Biotech) equilibrated in the same buffer, and the first, highly UV-absorbing flow-through peak was collected. This fraction was stirred with 1 ml of Pro-Bond nickel chelate resin at 4 °C for 2 h. The resin was then loaded onto a column, washed with 10 ml of the same buffer, and then eluted with the same buffer containing 500 mM imidazole. Fractions containing HMT2 were pooled, subjected to several cycles of dilution with imidazole-free buffer, and concentrated by ultrafiltration (Centricon 30). At each step in the procedure, sulfide:quinone reductase activity copurified with anti-HMT2 immunoreactive protein peaks. The final preparation, which showed an ~180-fold enrichment of enzyme specific activity, was adjusted to 50% glycerol and stored at -20 °C.

**HMT2 Activity Assay**—Sulfide:quinone oxidoreductase activity was measured under air at room temperature. A typical 250- $\mu$ l reaction contained 20 mM Tris-Cl, pH 7.8, 40  $\mu$ M coenzyme  $Q_2$  (Sigma), and 0.5  $\mu$ g of purified HMT2, to which 400  $\mu$ M  $Na_2S$  was added to begin the reaction. Reduction of  $Q_2$  was measured by loss of 285 nm absorption. The decrease in  $A_{285}$  was followed for 30 s and was linear during this period for all experiments. The mM extinction coefficient " $\Delta\epsilon$  oxidized-reduced" of  $Q_2$ , determined empirically by comparing the absorption of oxidized and  $NaBH_4$ -reduced  $Q_2$  samples in reaction buffer at 285 nm, was 8.85.  $S^{2-}$  from aliquots of reaction mixtures was trapped in 1 M zinc acetate and quantified by the methylene blue assay as described (14). Mitochondria, adjusted to 8  $\mu$ g of protein in 250  $\mu$ l, were assayed as above, except reactions contained 3.2 mM  $Na_2S$  and 2 mM KCN.

## RESULTS

**Mutant Phenotype**—*S. pombe* mutant strain JS563 bears a cadmium-hypersensitivity trait that segregates as a single locus. As this locus affects heavy metal tolerance, it was given the genetic designation *hmt2*. When compared with the wild-type parent strain JS21, which can grow at up to 800  $\mu$ M cadmium, the *hmt*<sup>-</sup> mutant ceases to grow at 100  $\mu$ M cadmium and shows reduced yield with as low as 5  $\mu$ M cadmium. A difference in growth rate was not found in the presence of high NaCl or sucrose concentrations, but a reduction relative to the wild type was observed after heat shock at 47 °C or in the presence of hydrogen peroxide, the thiol-oxidizing agent diamide, or the nonfermentable substrate glycerol. Because the catabolism of glycerol requires a functional respiratory pathway, the defect was suspected to be associated with mitochondrial function.

**Sulfide Hyperaccumulation and Hypersensitivity**—A noticeable trait of the mutant is that the colonies turn bright yellow in the presence of cadmium, suggesting the formation of CdS. Over an 18-h period, JS563 accumulated >6-fold as much acid-labile sulfide as the wild-type JS23 (Table I). *S. pombe* is known to increase sulfide production during cadmium stress, and a higher level of sulfide production was observed in both strains grown in 200  $\mu$ M cadmium, but the *hmt*<sup>-</sup> JS563 continued to exceed wild-type levels. Exogenous sulfide is toxic to *S. pombe* at concentrations in the 100  $\mu$ M range. Because the

TABLE I  
Genetic control of sulfide accumulation

$S^{2-}$  accumulation over 18 h of growth in minimal (SG) or complete (YG) medium, in the presence or absence of cadmium. Strains used are wild-type (JS23), *hmt2* disruption (JV5) or missense (JS563) mutant, sulfite reductase mutant (DS31), and *hmt2*<sup>-</sup>/sulfite reductase double mutant (JV3). Where indicated, the strains harbor the empty vector (pART1) or a complementing clone (pJV26). Normalized to the value obtained from the wild type grown in the absence of cadmium.

Strain	Plasmid	Media	Normalized $S^{2-}$	
			0 $\mu\text{M}$ Cadmium	200 $\mu\text{M}$ Cadmium
JS23	pART1	SG	1	3.2 ( $\pm 0.8$ )
JS563	pART1	SG	6.8 ( $\pm 3.1$ )	9.8 ( $\pm 3.8$ )
JS563	pJV26	SG	1.6 ( $\pm 0.09$ )	3.6 ( $\pm 1.6$ )
JV5		SG	8.4 ( $\pm 1.3$ )	15.2 ( $\pm 4.0$ )
JS23		YG	1	
JS563		YG	6.4 ( $\pm 0.5$ )	
DS31		YG	0.4 ( $\pm 0.04$ )	
JV3		YG	1.1 ( $\pm 0.05$ )	

*hmt2*<sup>-</sup> mutant already exhibits an elevated level of endogenous sulfide, it could be more sensitive to an exogenous supply of this substance. JS563 showed impaired growth relative to the wild-type strain in the presence of  $\text{Na}_2\text{S}$ , with the greatest differential observed at 200  $\mu\text{M}$   $\text{Na}_2\text{S}$ .

**Defect Not in Sulfate Assimilation**—One described route of sulfide production in *S. pombe* is the sulfur assimilatory pathway, where inorganic sulfur is routed from sulfate to sulfite to sulfide and then to cysteine. A defect in this pathway might increase the sulfide pool through either attenuating sulfide incorporation to cysteine or by overproducing sulfide directly. Both possibilities were examined by the following experiments. First, when cultured in minimal medium, JS563 grew as well as the wild type, suggesting that cysteine production is sufficient for cell growth. Further supplementation with cysteine (100  $\mu\text{M}$ ) did not increase its growth rate. Therefore, a defect in the incorporation of  $S^{2-}$  into cysteine seems unlikely.

Second, if sulfide overaccumulation were because of hyperactivity in sulfate assimilation, a genetic block in this pathway should abolish sulfide hyperaccumulation. The double mutant JV3 contains mutations in both *hmt2* and sulfite reductase. Like the parent sulfite-reductase mutant strain DS31, JV3 is unable to convert sulfate to cysteine and therefore requires cysteine supplementation. For this reason, sulfide assays were carried out on cells grown in the complete YG medium. DS31 accumulated far less sulfide than either wild-type or JS563 (Table I), as expected from its lack of sulfite reductase activity. However, DS31 also accumulated  $\sim 3$ -fold less sulfide than JV3, suggesting that the *hmt*<sup>-</sup> locus in JV3 enhances sulfide accumulation through a pathway separate from inorganic sulfur assimilation.

**Kinetics of Sulfide Consumption**—To address if the *hmt2*<sup>-</sup> mutation affects the consumption of  $S^{2-}$ , cells were pulse-labeled with  $^{35}\text{SO}_4^{2-}$ . During the brief 15-min labeling period, both wild-type and mutant cells converted  $^{35}\text{SO}_4^{2-}$  into  $^{35}\text{S}^{2-}$  (Fig. 1, time = 0 h). Most of this  $^{35}\text{S}^{2-}$  then disappeared, as it was incorporated into organic sulfur compounds, leaving approximately equal amounts in mutant and wild-type cells after 2 h. Over the next 20 h, wild-type cells gradually turned over this pool of  $^{35}\text{S}^{2-}$ , but in the *hmt2*<sup>-</sup> mutant this pool was not depleted. During that time, total (radioactive plus nonradioactive) sulfide levels accumulated more rapidly in the mutant than in wild type (Fig. 1, inset). The pattern indicates that the *hmt2*<sup>-</sup> defect lowers the consumption of the sulfide pool. This alone may account for the higher accumulation of sulfide, although the data do not rule out the possibility that the mutation also enhanced *de novo*  $S^{2-}$  synthesis.

**Isolation of *hmt2*<sup>+</sup> Gene**—JS563 was transformed with a *S.*

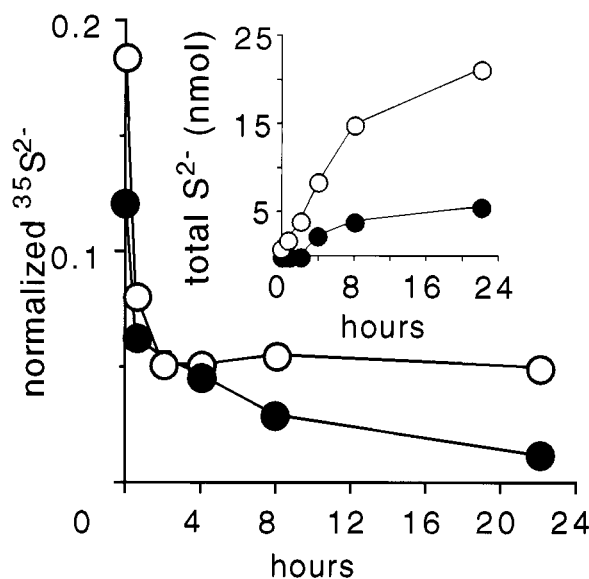


FIG. 1.  $S^{2-}$  turnover and accumulation. HPLC measurements of extracts from cadmium-induced wild-type (JS23, filled circles) and mutant (JS563, open circles). At each time point, 4 ml of radiolabeled culture was analyzed simultaneously for radioactive (main panel) and total (inset) sulfide. Normalized  $^{35}\text{S}^{2-}$  is the amount of radiolabeled sulfide at each time point divided by total  $^{35}\text{S}$  present in the cell at time 0.

*pombe* genomic library. A single plasmid clone, pJV1, with an 8.5-kb insert, restores cadmium tolerance to the mutant (Fig. 2). A deletion analysis of the 8.5-kb insert showed that a 1.9-kb *SalI/ScaI* subclone, in pJV26, complements the poor growth of the mutant on cadmium, hydrogen peroxide, diamide, or glycerol as well as restores wild-type sulfide levels (Table I). The 1.9-kb genomic fragment was used to isolate a 1834-base pair cDNA. In Northern blots, wild-type and mutant cells showed a single band of  $\sim 1.9$  kb that hybridizes to the *hmt2*<sup>+</sup> cDNA (Fig. 3A). Accumulation of this transcript increased by  $\sim 2$ -fold when cells were exposed to 200  $\mu\text{M}$  cadmium (Fig. 3B).

**An Engineered Gene Disruption**—To test whether the cloned DNA represented a wild-type allele of the genetic lesion or an extragenic suppressor, the wild-type allele was disrupted through integration of a *S. cerevisiae*  $\text{URA3}^+$  marker (Fig. 2). Polymerase chain reaction and Southern analysis indicated that, in the disruption strain JV5, the coding region of the gene is intact, but two copies of the disruption construct have integrated in tandem upstream of the *hmt2* coding region, disrupting the promoter and possibly part of the untranslated leader sequence. As a result, the 1.9-kb mRNA is deficient in JV5 (Fig. 3B). A shorter transcript in JV5 can be attributed to the truncated *hmt2* gene on the disruption construct itself because this band is also present in JV11, a strain bearing a random integration of the disruption construct. An additional transcript in JV5 of  $\sim 4$  kb hybridizes faintly to both  $\text{URA3}^+$  (not shown) and *hmt2*<sup>+</sup> probes. This band might represent transcriptional read-through from the upstream  $\text{URA3}^+$  gene through *hmt2*. Neither transcript detected in JV5 is expected to yield a functional *hmt2*<sup>+</sup> product.

The disruption phenotype in JV5 is very similar, though not identical, to that of the original mutant. As with JS563, JV5 is hypersensitive to cadmium, hyperaccumulates sulfide (Table I), and exhibits poorer growth after heat shock, or in the presence of hydrogen peroxide or  $\text{Na}_2\text{S}$ . Surprisingly, no significant difference is observed in the presence of diamide or with glycerol as the major carbon source. This anomaly could be attributed to a leaky allele. For example, the transcription of a functional mRNA in JV5, though severely reduced, might not

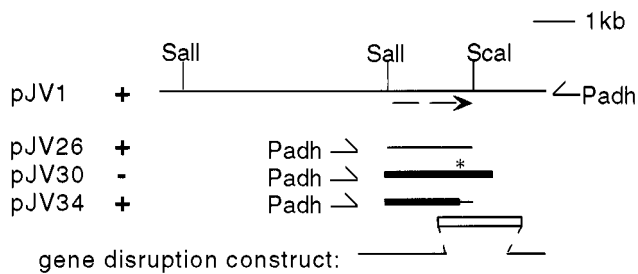


FIG. 2. **Genetic analysis of *hmt2*<sup>+</sup>.** Deletion derivatives of the complementing genomic clone pJV1 were transformed into JS563 and scored for their ability to complement (+) the mutant phenotype. The alcohol dehydrogenase promoter (Pdh) of the pART1 expression vector is indicated, and lies upstream of the *hmt2* coding region in pJV26, pJV30, and pJV34. The gene disruption construct shown is the *Xba*I fragment of pJV17, described under "Experimental Procedures." *Thin line*, wild-type genomic DNA; *thick line*, JS563 genomic DNA; *dashed arrow*, *hmt2*<sup>+</sup> cDNA; *open box*, *URA3*<sup>+</sup> insert; *asterisk*, site of mutation in JS563.

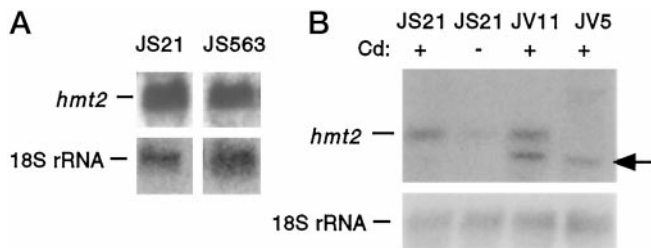


FIG. 3. **Northern analysis of *hmt2*<sup>+</sup> expression.** A, wild-type (JS21) and mutant (JS563) strains (harboring pART1) were grown in SG and exposed to 200  $\mu$ M cadmium for 24 h. 30  $\mu$ g total RNA from these cultures was hybridized with *hmt2*<sup>+</sup> cDNA, and rehybridized with a probe specific to the 18S rRNA. B, 30  $\mu$ g total RNA from a wild-type strain (JS21), a strain bearing a random insertion of the *hmt2* disruption construct (JV11), and the *hmt2* disruption strain (JV5) was hybridized to the *hmt2*<sup>+</sup> cDNA and to an 18S rRNA probe. Cells were or were not exposed to cadmium (200  $\mu$ M cadmium for 24 h) as indicated. The arrow marks the position of the truncated *hmt2* transcript originating from the disruption construct itself.

be entirely abolished. When JV5 was crossed to wild-type, the disruption phenotype segregated as a single locus and was linked with the *URA3*<sup>+</sup> marker (53 cadmium-hypersensitive, yellow, *URA3*<sup>+</sup> progeny: 46 cadmium-resistant, white, *URA3*<sup>-</sup> progeny,  $\chi^2 = 0.64$ ). When crossed to JS563, wild-type recombinants were not recovered (49 cadmium hypersensitive, yellow, *URA3*<sup>+</sup> progeny: 51 cadmium hypersensitive, yellow, *URA3*<sup>-</sup> progeny,  $\chi^2 = 0.04$ ). This genetic linkage between the original mutant locus and the disruption locus is consistent with the cloned gene corresponding to the genetic lesion in JS563.

**Sequence Change from *hmt2*<sup>+</sup> to *hmt2*<sup>-</sup>**—The *hmt2*<sup>+</sup> genomic and cDNA clones were sequenced on both DNA strands. *hmt2*<sup>+</sup> contains a putative 5' untranslated region of 357 nucleotides, longer than average for *S. pombe* (24). This region contains multiple poly-T and poly(A) stretches. The putative start methionine occurs at position 358, embedded in the sequence taaaatgt, which matches the most commonly observed *S. pombe* translational start motif at 8 of 9 positions (25). Comparison of genomic and cDNA sequences reveals that *hmt2*<sup>+</sup> lacks introns. The deduced *hmt2*<sup>+</sup> open reading frame is predicted to encode a protein of 459 amino acids, with a molecular mass of 51,574 Da and an isoelectric point of 9.5–10.

The mutant allele was cloned and sequenced across the entire coding region. Comparison with the wild-type sequence revealed a G to A transition that changed amino acid 396 from glutamate to lysine. When the mutant allele, in the vector pART1, is reintroduced into JS563, it is unable to complement

(Fig. 2, pJV30). When a 300-base pair region surrounding amino acid 396 is replaced by wild-type sequence, the hybrid allele is fully functional (Fig. 2, pJV34). This result demonstrates that this single point mutation is sufficient to account for the mutant phenotype.

**Similar Genes**—BLAST searches (26) of protein and nucleotide sequence data bases found sequence similarity between the encoded protein, HMT2, and a variety of oxidoreductases, some of which are listed in Table II. The two best matches, *C. vinosum* flavocytochrome c (6, 27) and *R. capsulatus* sulfide quinone reductase (28), are bacterial enzymes that oxidize sulfide. Overall sequence identity between HMT2 and these two enzymes is low (~20%). However, potentially functional features are conserved among these sequences (Fig. 4; and see the Discussion).

The sequences with greater similarity to HMT2 have unknown function. Apparent full-length genes from human, mouse, *Caenorhabditis elegans*, and the cyanobacterium *Synechocystis* sp. PCC6803 all appear to have > 30% overall sequence identity with HMT2. A fragmentary expressed sequence tag (EST) from rat appears similarly well conserved. ESTs from *Drosophila*, *Chloroflexus*, and *Schistosoma* all have >20% identity with HMT2. These proteins are predicted to have unusually high pI: human, pI ~ 9.5; mouse, pI ~ 9.1; *C. elegans*, pI ~ 9.8; *Synechocystis*, pI ~ 8.9. This feature is shared with HMT2 (pI ~ 9.9), sulfide quinone reductase (pI ~ 9.5), and NADH dehydrogenase (pI ~ 9.4).

**Mitochondrial Localization**—The N-terminal 24 amino acids of HMT2 display features characteristic of mitochondrial targeting sequences (29). The PSORT protein-targeting analysis program predicted with up to a 59% probability that HMT2 might be directed to mitochondria (30). In fission yeast extracts, a single anti-HMT2 immunoreactive band shows an apparent molecular mass of ~48 kDa. Abundance of this protein band correlates to *hmt2* mRNA accumulation. It is found in both *hmt2*<sup>+</sup> and in *hmt2*<sup>-</sup> (JS563) cells, is more abundant in cells containing *hmt2*<sup>+</sup> on a multicopy plasmid, and is barely detectable in cells containing a disruption of the *hmt2* promoter (JV5). The data are consistent with the 48-kDa band being the translation product of the *hmt2*<sup>+</sup> gene. The ~3-kDa reduction from the predicted size of HMT2 is consistent with the presumed cleavage of the putative mitochondrial targeting sequence during translocation from cytoplasm to mitochondria.

The bulk of HMT2 immunoreactive protein is pelleted by 100,000  $\times$  g centrifugation (Fig. 5A), suggesting that HMT2 is membrane-associated or enclosed within an organelle. In purified mitochondrial fractions (6-fold enriched in cytochrome oxidase specific activity), HMT2 is >5-fold enriched (Fig. 5B). A mitochondrial localization for HMT2 was supported by immunofluorescence microscopy experiments (not shown). The mitochondrial fractions were further subfractionated at pH 7.4. The mitochondrial membrane-enriched, fumarase-depleted (0.5 $\times$ ) pellet showed increased immunoreactivity for HMT2, suggesting that HMT2 may be membrane-associated (Fig. 5C). HMT2 is not predicted to have any hydrophobic regions capable of forming transmembrane helices. However, subfractionation at pH 11 increases the yield of soluble HMT2 (Fig. 5D). This property is characteristic of some peripheral membrane proteins.

**HMT2 Purification**—To facilitate purification of HMT2, a gene fusion construct, pJV40, was made to encode a modified HMT2 protein with additional histidine residues. This construct was able to complement fully the *hmt2*<sup>-</sup> mutant phenotype, suggesting that the additional amino acid residues do not interfere with the *in vivo* activity of the protein. We therefore assumed that the His<sub>6</sub>-tagged protein is suitable material for

TABLE II  
Sequence similarity to HMT2

Deduced proteins having significant primary sequence similarity to HMT2 ( $p < 0.05$  in BLAST searches of the protein and nucleotide data bases) are listed, together with the degree of pairwise amino acid identity with HMT2.

Organism	Function	Length (amino acids)	Identity (%)	Accession
<i>R. capsulatus</i>	Sulfide quinone reductase	Full (425)	20.2	EMB X97478
<i>C. vinosum</i>	Flavocytochrome <i>c</i>	Full (431)	20.2	SP Q06530
<i>E. coli</i>	NADH dehydrogenase	Full (434)	19.8	EMB V00306
<i>S. cerevisiae</i>	Glutathione reductase	Full (467)	15.6	GB L35342
<i>H. sapiens</i>	Unknown	Full (450)	38.4	Various <sup>a</sup>
<i>M. musculus</i>	Unknown	Full (452)	37.2	Various <sup>b</sup>
<i>Synechocystis</i> sp.	Unknown	Full (409)	36.2	DBJ 90907
<i>C. elegans</i>	Unknown	Full (423)	32.6	Various <sup>c</sup>
<i>R. norvegicus</i>	Unknown	Partial (141)	37.6	DBJ C06990
<i>C. aurantiacus</i>	Unknown	Partial (115)	27.0	EMB Z34000
<i>S. mansoni</i>	Unknown	Partial (61)	21.3	GB T24144
<i>D. melanogaster</i>	Unknown	Partial (143)	20.9	GB AA438562

<sup>a</sup> GB T74801, T64084, T85836, T86387, T95375, R50203, R40496, R13065, N50841, T64005, T74688, T95295, T98225, AA280758, AA281439, W96028, AA100857, AA083029, AA082940, AA057016, AA133917, W94661, AA253283, W15319, N54246, AA056968, N58703, AA486172, AA486109, AA526991, AA527252, AA576059; GB T27349; DBJ D82703, D82662; EMB Z19305; EMB D20113; GB T36144, AA353040, AA359423, AA385681, AA359712, AA353447, AA315963, AA383720, AA361822, AA382189, and EST 112244, 151798, 126925, 172344. The full sequence has been deposited in GenBank, with accession number AF042284.

<sup>b</sup> GB AA222168, AA184667, AA124108, AA266579, AA089176, AA106635, AA146443, AA245215, AA245216, AA208338, AA509391, AA434617, AA544472, AA499804, AA492716, AA473822.

<sup>c</sup> GB T00051, EMB Z82265, DBJ C38797.

initial biochemical characterization. The final protein preparation consisted of two major bands of ~52 and ~50 kDa, both of which were immunoreactive with anti-HMT2 antibodies. The smaller band may result from an alternative translation start site or may be a degradation product of the full-length protein.

**Flavin Binding**—Sequence analysis predicted that HMT2 might bind FAD. The purified protein from *E. coli* was visibly yellow, and light spectroscopy revealed absorption maxima at ~375 and ~455 nm in addition to the main protein peak at 280 nm (Fig. 6A). This profile is characteristic of a flavoprotein. Similar flavin absorption peaks are visible in free FAD (Fig. 6B). Free flavins exhibit fluorescence, with excitation maxima at ~375 and ~450 nm and an emission maximum at 520 nm. Although the purified protein was nonfluorescent, boiling for 3 min denatured the protein and released a soluble component having the fluorescence profile expected of a flavin. This indicates that the protein binds flavin noncovalently and that the fluorescence is quenched *in situ*.

Analysis of the fluorescence properties of the dissociated flavin (31) indicated that it consists predominantly of flavin adenine dinucleotide (93%); traces of FMN may represent breakdown products. Although sequence analysis predicts a 1:1 molar ratio of FAD to polypeptide, we experimentally obtained a ratio of ~1:3. This discrepancy may be because of incomplete binding of flavin in the heterologous expression system, losses of flavin during purification, or truncation of the protein.

**Sulfide:Quinone Oxidoreductase Activity**—The addition of sulfide caused rapid bleaching of the 450-nm absorption peak in HMT2 (Fig. 6A), but not in free flavin (Fig. 6B) or in another flavoprotein, glutathione reductase (not shown). The bleaching of HMT2 could be reversed when the sulfide was removed by ultrafiltration. This reversible bleaching is consistent with the reduction of the flavin by sulfide. The sequence similarity of HMT2 to sulfide-oxidizing enzymes, and the sensitivity of its absorption profile to sulfide, suggested that it might be capable of using sulfide as a substrate in a redox reaction. By analogy with the activity of the *R. capsulatus* sulfide quinone reductase, we tested the ability of HMT2 to catalyze the reaction  $S^{2-} + \text{coenzyme } Q_{2(\text{oxidized})} \rightarrow [S_{(\text{oxidized})}] + \text{coenzyme } Q_{2(\text{reduced})}$ . Coenzyme  $Q_2$  is a water-soluble ubiquinone analogue whose oxidized (Fig. 7A, a) and reduced (Fig. 7A, b) forms can be distinguished by their absorption profiles in the UV range. Addition of sulfide to a cuvette containing coenzyme  $Q_2$  and purified recombinant HMT2 causes a rapid decrease in the 285-nm

peak (Fig. 7B, b). The reaction between coenzyme  $Q_2$  and sulfide in the absence of HMT2, or in the presence of an equivalent quantity of free FAD ( $0.43 \pm 0.08$  nmol/min), is nearly 8-fold slower than the enzyme-catalyzed rate ( $3.35 \pm 0.54$  nmol/min, significant at  $p < 0.05$ ).

**Substrate Specificity**—We tested the ability of other electron acceptors to replace coenzyme  $Q_2$  in the HMT2-catalyzed reaction. Sulfide reacts rapidly and spontaneously with cytochrome *c*, 2,6-dichloroindophenol, and ferricytochrome, and the addition of HMT2 did not increase reaction rates. Sulfide fails to reduce menadione,  $NAD^+$ , or  $NADP^+$  spontaneously, and HMT2 was unable to stimulate these reactions. Likewise, sulfite, thiosulfate, cysteine, glutathione,  $\beta$ -mercaptoethanol, succinate, and pyridine nucleotides were all unable to replace sulfide in the HMT2-catalyzed reduction of  $Q_2$ . Therefore, HMT2 appears to possess a specific sulfide:quinone oxidoreductase activity.

**Reaction Stoichiometry**—Sulfide and oxidized quinone concentrations were determined independently at the end of a 10-min reaction of 50 nmol each of sulfide and coenzyme  $Q_2$  with 5  $\mu$ g of purified HMT2. Sulfide and oxidized quinone were consumed in an approximately 1:1 molar ratio ( $7.85 \pm 1.45$  nmol  $S^{2-}/7.6 \pm 0.99$  nmol quinone,  $n = 2$ ). Because flavoproteins and quinones both commonly carry two electrons, the stoichiometry of the reaction suggests that sulfide is oxidized to elemental sulfur and donates two electrons to coenzyme  $Q_2$ .

**Kinetic Parameters**—The sulfide-quinone reaction catalyzed by HMT2 is saturable with increasing concentrations of substrate; the apparent  $K_m$  for coenzyme  $Q_2$  is 2 mM. It is important to note that coenzyme  $Q_2$  is a water-soluble analogue of the more likely physiological electron acceptor, ubiquinone, and therefore the  $K_m$  obtained may not reflect the affinity of HMT2 for its true substrate. Additionally, because of the insolubility of high quinone concentrations in the reaction buffer, it was not possible to assay  $K_m$  for sulfide under saturating concentrations of quinone. At lower quinone concentrations (40  $\mu$ M),  $K_m$  for sulfide was calculated to be 2 mM. Using saturating  $S^{2-}$  (3 mM) and the highest concentration of quinone (1.5 mM) that can be assayed, we obtained an apparent  $V_{\text{max}}$  of 1.36  $\mu$ M coenzyme  $Q_2$  reduced per  $s$ - $\mu$ g of enzyme, and  $k_{\text{cat}}$  of 52/sec (assuming an active enzyme concentration of 22.3 nM, based on incomplete FAD binding).

**Sulfide:Quinone Oxidoreductase Activity in Mitochon-**

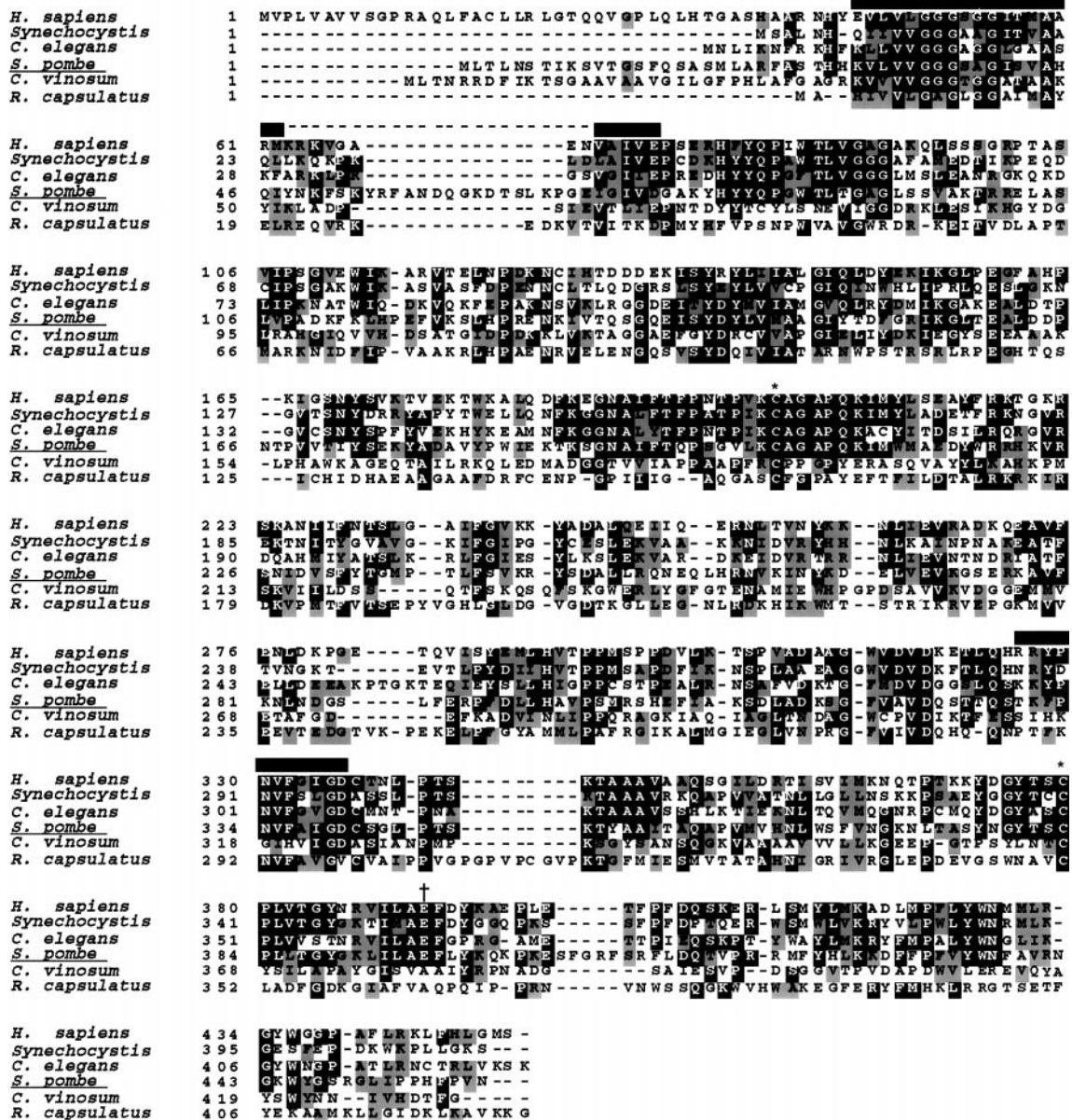


FIG. 4. Sequence alignment of HMT2 with putative homologues. Multiple sequence alignment of HMT2 from *S. pombe* (underlined) with putative distant homologues from *C. vinosum* and *R. capsulatus* and putative near homologues from *Homo sapiens*, *Synechocystis* sp. PCC6803, and *C. elegans*. Residues that are identical (black shading) or similar (gray shading) among at least three of the sequences are highlighted. The bipartite FAD-binding motif is indicated by black bars; the putative redox-active cysteines, by asterisks; and the site of the missense mutation in JS563, by a cross.

*dria*—We tested the native protein in its physiological context for the ability to carry out the same reaction. Mitochondria were isolated from wild-type (JS23) and mutant (JS563) cells. The specific activity of fumarase, an enzyme of the mitochondrial matrix, was equivalent in the two preparations. Mitochondria from both strains were able to reduce exogenous coenzyme Q<sub>2</sub> at low rates in the absence of added electron donor (JS23: 75 ± 51 nmol/min·mg; JS563: 68 ± 23 nmol/min·mg). The addition of sulfide significantly increased the rate of quinone reduction in JS23 mitochondria, and the spectrum of the reaction mixture showed a rapid decrease in the 285-nm absorption peak (Fig. 7C, b). Sulfide:quinone reductase activity, corrected for the background rate of quinone reduction, is significantly higher in JS23 (144 ± 45 nmol/min·mg) than in JS563 mitochondria (21 ± 12 nmol/min·mg, *p* < 0.05). Therefore, fission yeast mitochondria possess a sulfide:quinone oxidoreductase activity that correlates to the presence of functional HMT2 protein.

## DISCUSSION

Purified recombinant HMT2 protein is ~25-fold enriched over isolated mitochondria in both protein abundance and in sulfide:quinone oxidoreductase-specific activity. This suggests that the activity of HMT2 itself could account for all of the sulfide:quinone oxidoreductase activity measured in fission yeast mitochondria. The apparent *K<sub>m</sub>* for sulfide is relatively high (2 mM), when determined with a water-soluble analogue of the more likely electron acceptor, ubiquinone. Assuming this value is physiologically meaningful, HMT2 could nonetheless be adequately supplied with substrate under such conditions as heavy metal exposure, when whole-cell sulfide levels can exceed 1 mM. Quinone should also be available, as ubiquinone is abundant in the mitochondrial inner membrane.

Key features are shared among HMT2 and two sulfide dehydrogenases, flavocytochrome *c* from *C. vinosum* and sulfide quinone reductase from *R. capsulatus*. Flavocytochrome *c* binds

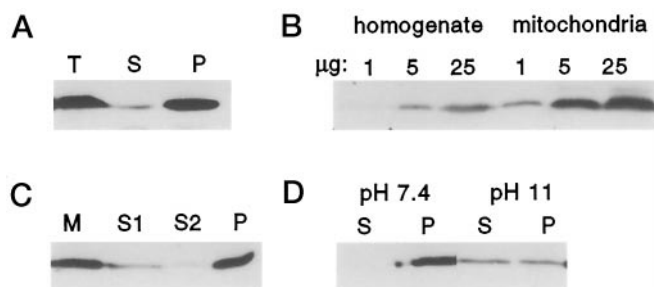


FIG. 5. **Western blots of cell fractions.** A, 30  $\mu\text{g}$  total protein (*T*), and the supernatant (*S*) and pellet (*P*) resulting from a 1-h,  $100,000 \times g$  centrifugation of an equivalent 30- $\mu\text{g}$  sample. B, 1, 5, or 25  $\mu\text{g}$  total protein from an initial *S. pombe* homogenate and from mitochondria purified from the same homogenate were blotted and probed with antibodies to HMT2. C, whole mitochondria (*M*) were osmotically shocked and divided into a supernatant fraction (*S1*) and a pellet. The pellet was sonicated and centrifuged to separate a second supernatant (*S2*) and pellet (*P*). Each lane contains 2.5  $\mu\text{g}$  of protein. D, whole mitochondria were sonicated at pH 7.4 or pH 11, then separated into supernatant (*S*) and pellet (*P*) fractions by centrifugation at  $100,000 \times g$  for 1 h. 2  $\mu\text{g}$  of protein from each fraction was blotted and probed with antibodies to HMT2.

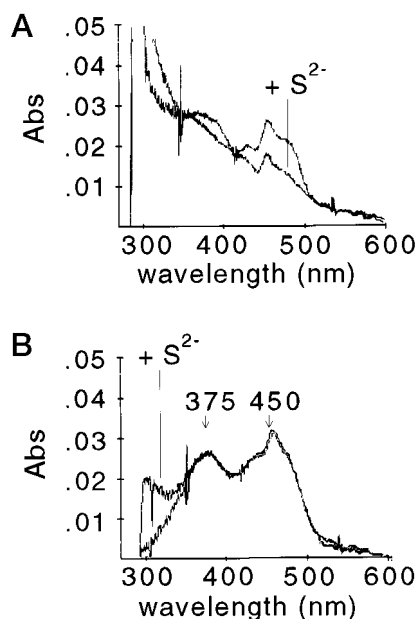


FIG. 6. **Absorbance spectra of HMT2 and FAD.** Absorbance spectra were recorded before and immediately after (+ $\text{S}^{2-}$ ) addition of 1.25 mM sulfide to purified HMT2 (A) or free FAD (B). Indicated are absorbance maxima (375 and 450 nm) of free FAD. Each sample was adjusted to 2.5  $\mu\text{M}$  flavin, assuming a mM extinction coefficient of 11.3 at 450 nm. After addition of sulfide, the increase of absorbance at  $\sim 230$  nm is because of sulfide itself.

a FAD cofactor via a two-part sequence motif (amino acids 34–64 and 314–324; Fig. 4, *black bar*) (6, 27) that is also present in sulfide quinone reductase and in HMT2. A pair of cysteines (amino acids 191 and 367; Fig. 4, \*) forming a disulfide bridge adjacent to the flavin in flavocytochrome *c* has been implicated to be catalytically involved in the redox reaction (6, 32). Aligning cysteines are also present in sulfide quinone reductase and in HMT2. Finally, the predicted secondary structure of HMT2 bears striking similarities with the known structure of flavocytochrome *c*. The similarity is greater than to any other protein in the Protein Data Bank as judged by the program PHDthreader (33). Previously, it has been suggested that all flavoenzymes known to be involved in sulfur chemistry may be related (27). HMT2 extends this family of related proteins to the eukaryotes.

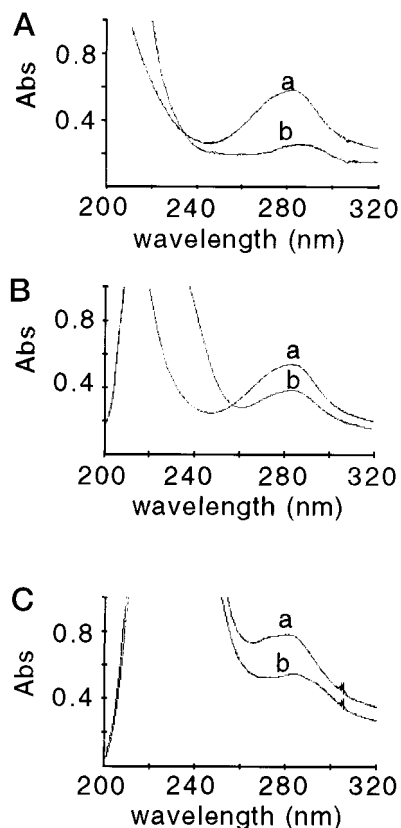


FIG. 7. **Absorbance spectra of oxidized versus reduced coenzyme  $\text{Q}_2$ .** A, absorbance spectra of 40  $\mu\text{M}$  coenzyme  $\text{Q}_2$  before (a) and after (b) chemical reduction with  $\text{NaBH}_4$ . B, absorbance spectra of reaction mixture containing 40  $\mu\text{M}$  coenzyme  $\text{Q}_2$  and 0.5  $\mu\text{g}$  of HMT2 before (a) and after (b) addition of 400  $\mu\text{M}$  sulfide. The additional absorbance at  $\sim 230$  nm is because of sulfide itself. C, absorbance spectra of a sulfide:quinone reaction catalyzed by mitochondria. Spectra were taken immediately after the addition of sulfide (a) and 4 min later (b).

It is possible that HMT2 functions in the detoxification of endogenous sulfide. Not all sulfide produced during the assimilation of inorganic sulfur is immediately incorporated into amino acids, and we can detect a low level of acid-labile sulfide even in wild-type cells. Sulfide is a potent inhibitor of cytochrome *c* oxidase (34), and accumulation of sulfide in mitochondria would be expected to poison respiration. Therefore, a mitochondrial sulfide dehydrogenase might play a role in ensuring that local sulfide concentration near cytochrome *c* oxidase is kept low. Consistent with this hypothesis, *hmt2<sup>-</sup>* cells grow poorly on a nonfermentable carbon source, suggesting that unchecked accumulation of sulfide may interfere with respiration. The exact role of HMT2 in cadmium tolerance is not yet clear, but a likely possibility is to detoxify excess sulfide generated during cadmium stress.

Mitochondrial sulfide oxidation is not unprecedented. Mitochondria of several species of marine animals have been shown to couple sulfide oxidation to the production of ATP (7, 9–12), but the proteins or genes responsible for the initial oxidation step have not been purified or cloned. In the lugworm *Arenicola marina*, electrons from sulfide appear to enter the electron transport chain at the level of ubiquinone (12), and the authors postulated that the enzyme involved might be similar to the sulfide quinone reductase of *R. capsulatus*. HMT2, a mitochondrial protein with homology to the *R. capsulatus* sulfide quinone reductase, strengthens this hypothesis by providing a genetic link between mitochondrial and bacterial sulfide oxidation. Intriguingly, genes similar to *hmt2<sup>+</sup>* appear in worms,

flies, mice, rats, and humans. A heat-labile sulfide oxidizing activity has been reported in rat liver mitochondria (35, 36). It is possible that the machinery for capturing electrons from sulfide has been conserved in evolution, although it has been adapted to new physiological roles.

*Acknowledgment*—We thank H. A. Koshinsky for assistance with the preparation of figures.

## REFERENCES

1. Brune, D. C., and Truper, H. G. (1986) *Arch. Microbiol.* **145**, 295–301
2. Shahak, Y., Arieli, B., Padan, E., and Hauska, G. (1992) *FEBS Lett.* **299**, 127–130
3. Van Beeumen, J., Van Bun, S., Meyer, T. E., Bartsch, R. G., and Cusanovich, M. A. (1990) *J. Biol. Chem.* **265**, 9793–9799
4. Arieli, B., Shahak, Y., Taglich, D., Hauska, G., and Padan, E. (1994) *J. Biol. Chem.* **269**, 5705–5711
5. Shahak, Y., Klughammer, C., Schreiber, U., Padan, E., Herrman, I., and Hauska, G. (1994) *Photosynth. Res.* **39**, 175–181
6. Chen, Z.-W., Koh, M., Van Driessche, G., Van Beeumen, J. J., Bartsch, R. G., Meyer, T. E., Cusanovich, M. A., and Mathews, F. S. (1994) *Science* **266**, 430–432
7. Oeschger, R., and Vismann, B. (1994) *Ophelia* **40**, 147–158
8. Oeschger, R., and Vetter, R. D. (1992) *Mar. Ecol. Prog. Ser.* **86**, 167–179
9. Lee, R. W., Kraus, D. W., and Doeller, J. E. (1996) *Biol. Bull.* **191**, 421–430
10. Bagarino, T., and Vetter, R. D. (1990) *J. Comp. Physiol. B Biochem. Syst. Environ. Physiol.* **160**, 519–527
11. Powell, M. A., and Somero, G. N. (1986) *Science* **233**, 563–566
12. Voelkel, S., and Grieshaber, M. K. (1996) *Eur. J. Biochem.* **235**, 231–237
13. Perego, P., Vande Weghe, J., Ow, D. W., and Howell, S. B. (1997) *Mol. Pharmacol.* **51**, 12–18
14. Speiser, D. M., Ortiz, D. F., Kreppel, L., Scheel, G., McDonald, G., and Ow, D. W. (1992) *Mol. Cell. Biol.* **12**, 5301–5310
15. Alfa, C., Fantes, P., Hyams, J., McLeod, M., and Warbrick, E. (1993) *Experiments with Fission Yeast: a Laboratory Course Manual*, pp. 134–135, Cold Spring Harbor Laboratory Press, Plainview, NY
16. Ortiz, D. F., Kreppel, L., Speiser, D. M., Scheel, G., McDonald, G., and Ow, D. W. (1992) *EMBO J.* **11**, 3491–3499
17. Beach, D., and Nurse, P. (1981) *Nature* **290**, 140–142
18. McLeod, M., Stein, M., and Beach, D. H. (1987) *EMBO J.* **6**, 729–736
19. Jault, J.-M., Comte, J., Gautheron, D. C., and Di Pietro, A. (1994) *J. Bioenerg. Biomembr.* **26**, 447–456
20. Moore, A. L., Walters, A. J., Thorpe, J., Fricaud, A.-C., and Watts, F. Z. (1992) *Yeast* **8**, 923–933
21. Daum, G., Bohni, P. C., and Schatz, G. (1982) *J. Biol. Chem.* **257**, 13028–13033
22. Bergmeyer, H. U., and Gawehn, K. (eds) (1974) *Methods of Enzymatic Analysis*, pp. 452–453, 2nd Ed., Vol. 1, Academic Press, Inc., New York
23. Schneppenheim, R., Budde, U., Dahlmann, N., and Rautenberg, P. (1991) *Electrophoresis* **12**, 367–372
24. Russell, P. (1989) in *Molecular Biology of the Fission Yeast* (Nasim, A., Young, P., and Johnson, B., eds), pp. 243–271, Academic Press, San Diego
25. Zhang, M. Q., and Marr, T. G. (1994) *Nucleic Acids Res.* **22**, 1750–1759
26. Altschul, S. F., Gish, W., Miller, W., Myers, E. W., and Lipman, D. J. (1990) *J. Mol. Biol.* **215**, 403–410
27. Van Driessche, G., Koh, M., Chen, Z.-w., Mathews, F. S., Meyer, T. E., Bartsch, R. G., Cusanovich, M. A., and Van Beeumen, J. J. (1996) *Protein Sci.* **5**, 1753–1764
28. Schutz, M., Shahak, Y., Padan, E., and Hauska, G. (1997) *J. Biol. Chem.* **272**, 9890–9894
29. von Heijne, G., Steppuhn, J., and Herrmann, R. (1989) *Eur. J. Biochem.* **180**, 535–545
30. Nakai, K., and Kanehisa, M. (1992) *Genomics* **14**, 897–911
31. Faeder, E. J., and Siegel, L. M. (1973) *Anal. Biochem.* **53**, 332–336
32. Meyer, T. E., Bartsch, R. G., and Cusanovich, M. A. (1991) *Biochemistry* **30**, 8840–8845
33. Rost, B. (1995) in *The Third International Conference on Intelligent Systems for Molecular Biology (ISMB)* (Rawlings, C., Clark, D., Altman, R., Hunter, L., Lengauer, T., and Wodak, S., eds), pp. 314–321, AAAI Press, Menlo Park, CA
34. National Research Council, Division of Medical Sciences, Subcommittee on Hydrogen Sulfide (1979) *Hydrogen Sulfide*, University Park Press, Baltimore
35. Bartholomew, T. C., Powell, G. M., Dodgson, K. S., and Curtis, C. G. (1980) *Biochem. Pharmacol.* **29**, 2431–2437
36. Baxter, C. F., Van Reen, R., Pearson, P. B., and Rosenberg, C. (1958) *Biochim. Biophys. Acta* **27**, 584–591